

Martyn P. Nash · Adam Wittek ·
Poul M. F. Nielsen · Magdalena Kobielarz ·
Anju R. Babu · Karol Miller *Editors*

Computational Biomechanics for Medicine

Towards Automation and Robustness
of Computations in the Clinic

 Springer

Computational Biomechanics for Medicine

Martyn P. Nash · Adam Wittek ·
Poul M. F. Nielsen · Magdalena Kobielarz ·
Anju R. Babu · Karol Miller
Editors

Computational Biomechanics for Medicine

Towards Automation and Robustness
of Computations in the Clinic

 Springer

Editors

Martyn P. Nash
Auckland Bioengineering Institute
University of Auckland
Auckland, New Zealand

Poul M. F. Nielsen
Auckland Bioengineering Institute
University of Auckland
Auckland, New Zealand

Anju R. Babu
Department of Biotechnology and Medical
Engineering
National Institute of Technology Rourkela
Rourkela, India

Adam Wittek
Intelligent Systems for Medicine
Laboratory
Department of Mechanical Engineering
The University of Western Australia
Perth, WA, Australia

Magdalena Kobielarz
Department of Mechanics, Materials
and Biomedical Engineering
Wroclaw University of Science
and Technology
Wroclaw, Poland

Karol Miller
Intelligent Systems for Medicine
Laboratory
Department of Mechanical Engineering
The University of Western Australia
Perth, WA, Australia

ISBN 978-3-031-34905-8 ISBN 978-3-031-34906-5 (eBook)
<https://doi.org/10.1007/978-3-031-34906-5>

© The Editor(s) (if applicable) and The Author(s), under exclusive license to Springer Nature Switzerland AG 2023

This work is subject to copyright. All rights are solely and exclusively licensed by the Publisher, whether the whole or part of the material is concerned, specifically the rights of translation, reprinting, reuse of illustrations, recitation, broadcasting, reproduction on microfilms or in any other physical way, and transmission or information storage and retrieval, electronic adaptation, computer software, or by similar or dissimilar methodology now known or hereafter developed.

The use of general descriptive names, registered names, trademarks, service marks, etc. in this publication does not imply, even in the absence of a specific statement, that such names are exempt from the relevant protective laws and regulations and therefore free for general use.

The publisher, the authors, and the editors are safe to assume that the advice and information in this book are believed to be true and accurate at the date of publication. Neither the publisher nor the authors or the editors give a warranty, expressed or implied, with respect to the material contained herein or for any errors or omissions that may have been made. The publisher remains neutral with regard to jurisdictional claims in published maps and institutional affiliations.

This Springer imprint is published by the registered company Springer Nature Switzerland AG
The registered company address is: Gewerbestrasse 11, 6330 Cham, Switzerland

Contents

Patient-Specific Model Generation

Generation of Patient-Specific Structured Hexahedral Mesh of Aortic Aneurysm Wall 3
Farah Alkhatib, George C. Bourantas, Adam Wittek, and Karol Miller

Workflow for Generating Personalised Anatomical Models of the Skeleton and the Skin Surface of the Upper Torso 23
Fangchao Pan, Kejia Khoo, Thiranjia P. Babarenda Gamage, Gonzalo Maso Talou, Poul M. F. Nielsen, and Martyn P. Nash

Automated Modeling of Brain Bioelectric Activity Within the 3D Slicer Environment 33
Saima Safdar, Benjamin Zwick, George Bourantas, Grand Joldes, Damon Hyde, Simon Warfield, Adam Wittek, and Karol Miller

Solid Biomechanics

Rapid Prediction of Breast Biomechanics Under Gravity Loading Using Surrogate Machine Learning Models 49
Max Dang Vu, Gonzalo D. Maso Talou, Huidong Bai, Poul M. F. Nielsen, Martyn P. Nash, and Thiranjia Prasad Babarenda Gamage

Effect of Analyst Segmentation Variability on Computed AAA Stress Distributions 63
Tim Hodge, Jasper C. Y. Tan, Paddy H. Koh, Eli Storer, Andy Huynh, Farah Alkhatib, Karol Miller, and Adam Wittek

The Effects of the Spine on the Analysis of Peak Wall Stress in Abdominal Aortic Aneurysms 79
Michael D. Liddelow, Farah Alkhatib, Adam Wittek, and Karol Miller

Analysis of Head Protection Performance of Bicycle Helmets by Full-Scale Computational Biomechanics Modelling of Real-World Car-to-Cyclist Accidents	95
Fang Wang, Ke Peng, Jiajie Yin, Shenghui Hu, Fan Li, and Lin Hu	
Fluid Biomechanics	
Modelling the Blood Flow and Drug Transport in an Anatomically Accurate Rat Liver	117
Harvey Ho, Chong Sheng Chuah, and Uta Dahmen	
Numerical Simulation of Blood Flow Under High Shear Forces in Experimental and Clinical Applications	125
Przemysław Kurtyka, Magdalena Kopernik, Ievgenii Altyntsev, Maciej Gawlikowski, Roman Kustos, Małgorzata Pomorska, Christoph Hofstetter, Juergen M. Lackner, and Roman Major	
Effect of Mechanical Aortic Valves on Coronary Artery Flow in a Patient Suffering from Ischemic Heart Disease	145
Anna Nieroda, Krzysztof Jankowski, and Marek Pawlikowski	
New Applications	
Stump Length Effect on Pelvic Tilt in Transfemoral Amputees Assessed by Statistical Parametric Mapping	161
Vít Nováček, Simona Bartošová, Bohumír Chládek, Pavel Jedlička, Alberto Sanchez-Alvarado, Ondřej Vyhnal, Tomáš Železný, Jiří Křen, and Luděk Hynčák	
Assessment of Obstructive Sleep Apnea Phenotypes from Routine Sleep Studies: A New Approach to Precision Medicine	173
Raichel M. Alex, Khosrow Behbehani, and Donald E. Watenpaugh	
Index	193

Patient-Specific Model Generation

Generation of Patient-Specific Structured Hexahedral Mesh of Aortic Aneurysm Wall



Farah Alkhatib, George C. Bourantas, Adam Wittek, and Karol Miller

Abstract Abdominal aortic aneurysm (AAA) is an enlargement in the lower part of the main artery “Aorta” by 1.5 times its normal diameter. AAA can cause death if rupture occurs. Elective surgeries are recommended to prevent rupture based on measurement of AAA diameter and diameter growth rate. Reliability of these geometric parameters to predict the AAA rupture risk has been questioned, and biomechanical assessment has been proposed to distinguish between patients with high and low risk of AAA rupture. Stress in aneurysm wall is the main variable of interest in such assessment. Most studies use finite element method to compute AAA stress. This requires discretising patient-specific geometry (aneurysm wall and intraluminal thrombus ILT) into finite elements/meshes. Tetrahedral elements are most commonly used as they can be generated in seemingly automated and effortless way. In practice, however, due to complex aneurysm geometry, the process tends to require time-consuming mesh optimisation to ensure sufficiently high quality of tetrahedral elements. Furthermore, ensuring solution convergence requires large number of tetrahedral elements, which leads to relatively long computation times. In this study, we focus on generation of hexahedral meshes as they are known to provide converged solution for smaller number of elements than tetrahedral meshes. We limit our investigation to already existing algorithms and software packages for mesh generation. Generation of hexahedral meshes for continua with complex/irregular geometry, such as aneurysms, requires analyst interaction. We propose a procedure for generating high-quality patient-specific hexahedral discretisation of aneurysm wall using the algorithms available in commercial software package for mesh generation. We demonstrate, for the actual aneurysms, that the procedure facilitates patient-specific mesh generation within timeframe consistent with clinical workflow while requiring only limited input from the analyst.

F. Alkhatib (✉) · G. C. Bourantas · A. Wittek · K. Miller
Intelligent Systems for Medicine Laboratory, The University of Western Australia, Perth, Western Australia, Australia
e-mail: farah.alkhatib@research.uwa.edu.au

K. Miller
Harvard Medical School, Boston, MA, USA

Keywords Abdominal aortic aneurysm · Structured hexahedral elements · Patient-specific aneurysm wall

1 Introduction

Abdominal aortic aneurysm (AAA) is a permanent and irreversible enlargement in the lower part of the aorta [1], the main artery that pumps blood from the heart to the rest of human body. It is a chronic vascular disease of elderly men (over 65 years old). Prevalence is regarded as negligible before the age of 55–60 years [2]. AAA prevalence in women is up to 4–6 times less than in men [3].

AAA is usually diagnosed incidentally by unrelated examination as it is a symptomless disease [2]. The most fatal event of AAA is rupture, where mortality rate can reach up to 90% [4] leading to 200,000 deaths annually worldwide [5] and around 1500 deaths yearly in Australia and the Oceania region [6].

According to current AAA management, patients undergo elective surgical intervention if their maximum aortic diameter is more than 55 mm for men and 50 mm for women [7, 8]. Below these recommended thresholds, patients are placed on surveillance program that monitors the aneurysm growth rate. The surgery is recommended if the growth rate exceeds 10 mm/year. Australia has a high rate of AAA repairs below these recommended thresholds compared to other Western countries. However, the probability for aneurysms with aortic diameter of 40–50 mm under surveillance to rupture is only 0.4% per year, which is lower than the risk of death due to the postoperative complications [2].

This raises the question of how to best manage AAAs as there is a balance between interventions to prevent AAA rupture versus overtreatment that may cause harm to patients and incur non-essential medical cost. Over the last 25 years, researchers introduced different AAA biomechanical rupture risk indicators or indices to identify patients at high risk of AAA rupture [9–13] and conversely those at low risk for whom surgical intervention can be avoided. Evaluation of such indices is beyond the scope of this study. Biomechanical indices for evaluating the AAA rupture risk strongly rely on computation of AAA wall stress [9]. Finite element method (FEM) dominates such computations. It requires discretising patient-specific geometry (aneurysm wall and intraluminal thrombus ILT) into finite elements/meshes to create a computational grid.

Patient-specific tetrahedral meshes are often used in computational biomechanics analysis of AAA as it is believed that such meshes can be created automatically with high element quality by analysts without expertise in computational grid generation [13, 14]. In a study by Miller et al. [15], AAA (aneurysm wall and ILT) finite element models contained more than 1 million tetrahedral elements. This high number of elements ensures convergent solution but tends to result in relatively long computational times. Furthermore, automated elimination of poor-quality tetrahedral elements typically requires application of mesh optimisation procedures. From our experience, presence of even small number of poor-quality elements may lead

to very long optimisation times (up to around 40–50 minutes of a personal computer with Intel quad-core i7 processor). Therefore, we focus on hexahedral meshes as they require a smaller number of elements than tetrahedral meshes [16]. For aneurysm walls discretised using 30,000–50,000 hexahedral elements, around 500,000 tetrahedral elements were needed to achieve similar geometric discretisation accuracy [17].

Generation of high-quality structured (mapped) hexahedral finite element meshes of healthy blood vessel walls can be done automatically by defining the vessels centre-lines [18–20] using freely available software such as pyFormex (<https://github.com/dladd/pyFormex>) and Gmsh (<https://gmsh.info/>). This, however, does not extend to complex/irregular geometry of AAAs. Generation of structured hexahedral meshes of AAAs tends to require expert's knowledge of finite element meshing procedures and substantial manual effort of the analyst. Specialised mesh generation code developed by Tarjuelo-Gutierrez et al. [21] facilitates construction of hexahedral meshes for aneurysm wall and thrombus including the bifurcations. It relies on connecting the extracted axial and longitudinal lines in the aneurysm from the manual magnetic resonance imaging (MRI) segmentation and the calculated aneurysm centreline. Need for substantial effort of the analyst was also reported in the studies using well-established commercial mesh generators. Application of CEM CFD 14.5 (Ansys Inc., USA) to create patient-specific hexahedral finite element meshes of aneurysm wall required 4–8 h of analyst's work per case [12, 22]. Mayr et al. [23] used CUBIT mesh generator (<https://cubit.sandia.gov/>) to create hexahedral elements for aortic aneurysms for fluid-structure interaction simulation. Distinct advantage of CUBIT is that it can automatically partition complex geometries into mappable volumes to build structured hexahedral mesh. CUBIT is available for the US government use only. However, its commercial version, Coreform Cubit (<https://coreform.com/products/coreform-cubit/free-meshing-software/>), has no such restriction. A4Clinics VASCOPS (<http://www.vascops.com>) software to biomechanically analyse AAA rupture risk creates a hexahedral aneurysm wall with a minimal user interaction. Their meshing algorithm limits any mesh refinement along the circumferential and axial directions of aneurysm wall and ILT, which creates one layer through wall thickness and coarse elements for thick ILT [24]. However, in several studies it has been argued that at least two elements across the AAA wall thickness are needed for converged solution in terms of stress computation [25]. Zhang et al. [16, 26] have successfully created unstructured hexahedral meshes from volumetric data (medical images as an example). Automated unstructured hexahedral elements for aneurysm wall and ILT using Harpoon (<http://www.sharc.co.uk/index.htm>) were done by Maier et al. [27]. Our experience indicates that unstructured hexahedral meshes may contain some poor-quality elements, in particular elements with very low (close to zero or even negative) Jacobian quality measure [26, 28].

In this study, we demonstrate a procedure to create a high-quality patient-specific structured hexahedral mesh of aortic aneurysm wall models using commercially

available mesh generators for stress computation in the aneurysm wall. We use tetrahedral elements for the intraluminal thrombus (ILT) because of its complex geometry. Accurate ILT stress analysis is not a variable of interest as an indicator of AAA rupture risk, further justifying the use of tetrahedral elements.

2 Methods

2.1 Patient's Data and Patient-Specific AAA Geometry

A contrast-enhanced computed tomography angiography (CTA) image data set of four abdominal aortic aneurysm (AAA) patients with an average maximum aortic diameter of 55 mm (standard deviation = 9 mm) was used to demonstrate the meshing techniques proposed and used in this work. The CTA images were acquired at Fiona Stanley Hospital (Murdoch, Western Australia, Australia) using SOMATOM Definition Flash CT Scanner (Siemens Healthineers AG, Forchheim, Germany). The spatial resolution (voxel size) of the CTA images is $0.625 \times 0.625 \times 1.5 \text{ mm}^3$. Patients gave their informed consent before acquiring the images according to the Declaration of Helsinki.

The patient-specific AAA geometries were segmented from the CTA images using the open-source medical image analysis package, 3D Slicer (<https://www.slicer.org/>) [29]. The contrast-enhanced images allowed an automated segmentation for the lumen (blood channel) using the threshold algorithm in 3D Slicer segmentation module. The aneurysm (wall and the intraluminal thrombus "ILT") needed some manual work to distinguish between the aneurysm and surrounding tissues. Figure 1 shows the segmented AAA for a Patient 1; the aneurysm wall is shaded in blue, and the ILT is in red. We assumed constant wall thickness of 1.5 mm for the aneurysm wall, as there is no reliable method to accurately determine AAA wall thickness solely from CTAs has been developed yet [30].

2.2 Generation of Patient-Specific AAA Computational Grids

2.2.1 Patient-Specific AAA Meshes

Different meshing tools and algorithms can be used to generate patient-specific hexahedral meshes of aneurysm wall as stated in Introduction. We initially attempted to use an in-house algorithm (implemented using MATLAB) that reconstructs the aneurysm geometry using the aortic centreline and maximum distances from this centreline to the aortic wall. This algorithm defines subdivided circles and ellipses orthogonal to the centreline ready to be connected using splines to form surface quadrilateral meshes. We faced two main issues with this early-stage algorithm, (1)

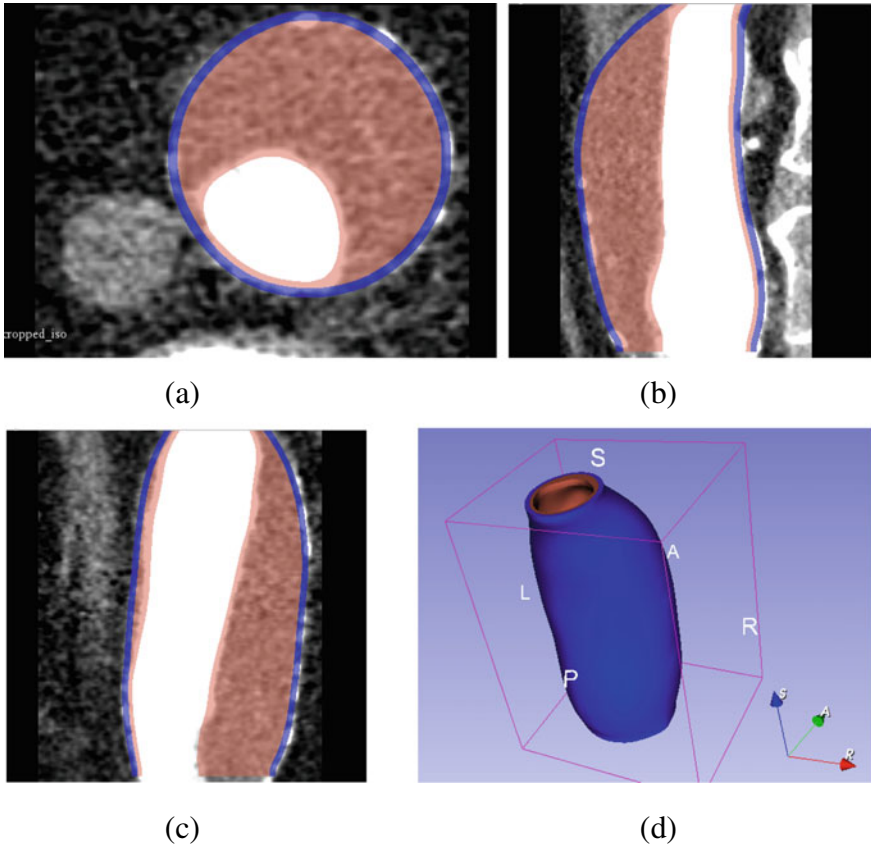
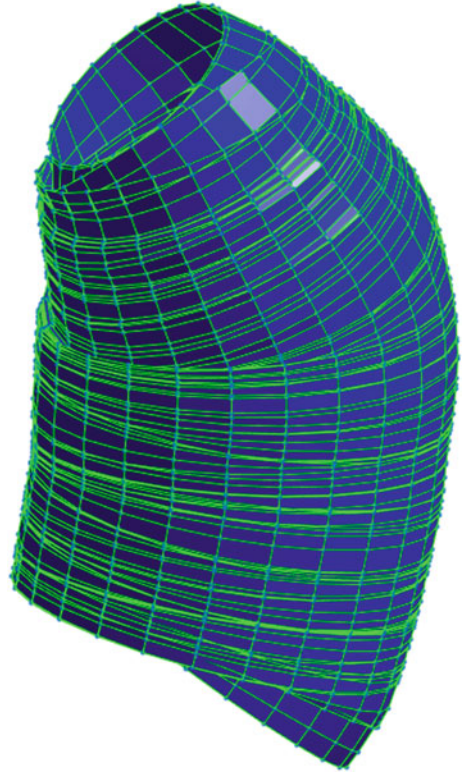


Fig. 1 Patient-specific abdominal aortic aneurysm (AAA) geometry obtained by segmentation of computed tomography angiography (CTA) images using 3D Slicer. The segmented aneurysm wall (constant thickness of 1.5 mm is assumed) is shown in blue, and the segmented intraluminal thrombus (ILT) is shown in red; **a** a slice from the axial view of AAA, **b** a slice from the sagittal view of AAA, **c** a slice from the coronal view of AAA, and **d** the 3D rendered AAA

the circles and ellipses may overlap in the locations that have a large change in wall curvature (Fig. 2), and (2) a smoothing technique (Laplace smoothing as an example [31]) should be used to improve the elements shape and mesh quality.

Fully automated hexahedral meshing was not possible for the aneurysm wall using known to us open-source and commercial mesh generators because of its irregular and asymmetrical shape. We initially used the mesh generator available in ABAQUS/CAE (<https://www.3ds.com/products-services/simulia/products/abaqus/>) finite element pre-processor. It provides high-quality element generation. However, it strongly relies on the user's expertise and requires substantial input (manual mesh generation work) from the user as the AAA geometry needs to be subdivided into many partitions in order to create a structured hexahedral mesh. In this study, we

Fig. 2 Example of surface meshing (2D quadrilateral elements) using a prototype in-house code showing the overlapped circles (green circles) created while defining the AAA geometry based on centrelines (Patient 1)



used the industrially applied mesh generation software Altair HyperMesh (<https://www.altair.com/hypermesh>) to create a high-quality hexahedral mesh of AAA wall. Our Intelligent Systems for Medicine Laboratory (ISML) team has many years of experience in using HyperMesh, and HyperMesh can be applied to generate high-quality meshes from computer-aided design (CAD) and image-derived geometries.

We imported the geometry of AAA wall extracted from the CTA images in stereo lithography (STL) format. Because of the irregular geometry of AAA, partitioning was needed to create the structured (mapped meshing) hexahedral mesh. Figure 3 shows the four aneurysm wall geometries meshed in this study.

The 3D hexahedral mesh (Fig. 4a) was created by sweeping the 2D meshed ring (Fig. 4b) along the aneurysm wall. The created 2D top ring of quadrilateral elements in the aneurysm wall defines the element size and number of hexahedral layers (elements) through wall thickness. We used two elements (size of 0.75 mm) through the wall thickness.

We created tetrahedral elements for the aneurysm intraluminal thrombus (ILT) using HyperMesh because of its complex shape. The transition between the quadrilateral surface meshes to tetrahedral volume meshes was important to create the shared conformal surface between the hexahedral aneurysm wall and the tetrahedral

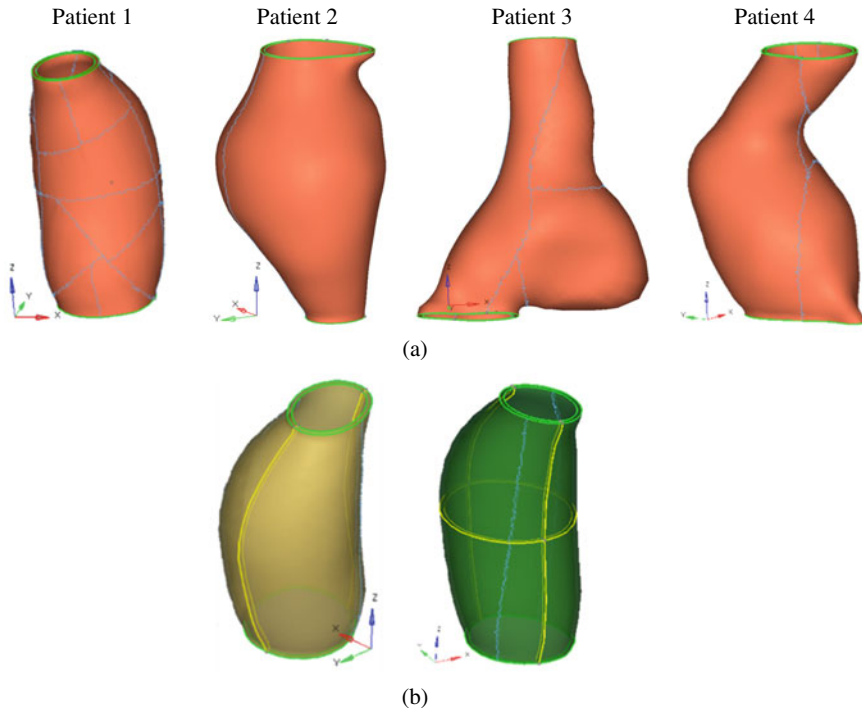


Fig. 3 **a** Aneurysm wall geometries for four patients extracted from computed tomography angiography (CTA) images and imported to HyperMesh finite element mesh generator in STL format. At least one partition was required before these geometries could be discretised (meshed) using hexahedral elements; **b** Partitioned aneurysm wall geometry (Patient 1) ready for mapped (structured) meshing: yellow shading—partition using one plane and green shading—partition using two planes. Bright yellow lines indicate the partitioning planes

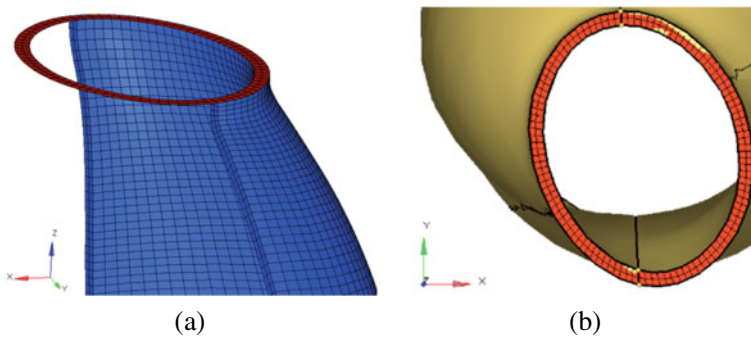


Fig. 4 Hexahedral meshing of aneurysm wall, **a** section of aneurysm wall (blue elements) showing the hexahedral meshes created by sweeping the quadrilateral 2D ring (red elements), and **b** top view of the aneurysm wall geometry that has the generated 2D top ring of quadrilateral elements used to create the 3D volume wall (hexahedral elements), element size is 0.75 mm

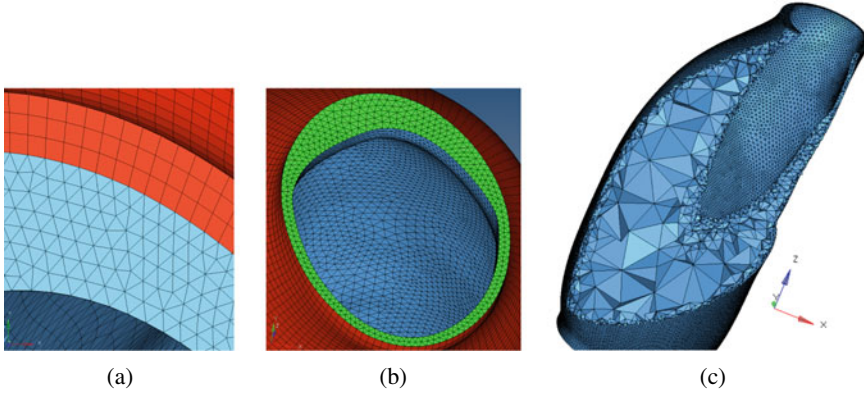


Fig. 5 Generation of tetrahedral intraluminal thrombus (ILT) mesh. **a** The top view of abdominal aortic aneurysm (AAA) showing the wall in red and ILT in blue, **b** 2D top edge created (green) to close the volume of ILT and generate the tetrahedral mesh, and **c** section view of the meshed ILT

ILT (Fig. 5a). We used the inner wall surface topology (nodes location) to create the outer surface of the ILT (triangular elements). We imported the inner surface of the ILT (the surface of the lumen segmented in 3D Slicer) and created a dummy mesh to close the top and bottom edges of the ILT creating water-tight surface assembly that defines the ILT (Fig. 5b). ILT tetrahedral mesh was then generated automatically while allowing the meshing algorithm to increase the element size in the areas distance from the surfaces defining the ILT boundary. This, in turned, reduced the number of elements and, hence, the computation time. We kept the nodes on the surfaces of wall and ILT fixed while allowing the splitting of quadrilaterals into triangles to avoid pyramid elements. The upper and lower edges (dummy mesh) were designated as freely adjustable nodes. A section view of the ILT tetrahedral mesh created in this study is shown in Fig. 5c.

2.2.2 Element Quality

Hexahedral meshes We used the following two measures to evaluate quality of hexahedral elements: (1) normalised/scaled Jacobian [26, 28] (a Jacobian value of 0.6 and higher is recommended [32]) and (2) the minimum and maximum allowable interior angles of a quadrilateral face (the suggested limits are between 45° and 135° [32])—see Fig. 6a for definition. Both measures need to be used as we found that some elements have high Jacobian, but their maximum or minimum interior angles are out of the recommended range. Figure 6a shows an example of such poor-quality element. We confirmed that such elements could be avoided by increasing the number of partitions or sections of the AAA geometry and by decreasing the element size.

Tetrahedral meshes We analysed quality of tetrahedral elements using the following two measures: (1) maximum and minimum allowable interior angle for

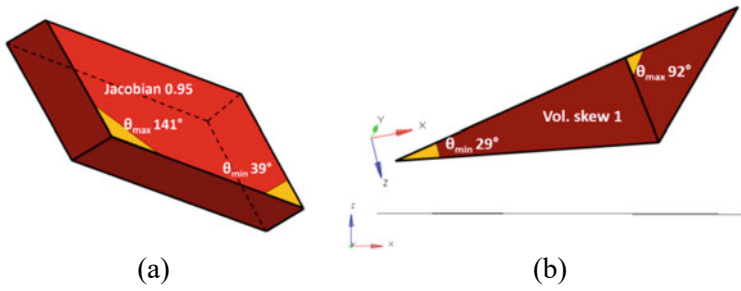


Fig. 6 Examples of poor-quality elements: **a** hexahedral element with Jacobian of 0.95, but with minimum interior angle of 39.25° and maximum interior angle of 141.36° that are out of the recommended allowable range of 45° – 135° [1]; and **b** two views of a “flat” tetrahedral element degenerated to triangle. Volumetric skew of this element equals one. Interior angles are highlighted in yellow

triangles [32] and (2) the volumetric skew [33]:

$$\text{Volumetric skew} = 1 - \frac{\text{Actual tetrahedron volume}}{\text{Ideal tetrahedron volume}}, \tag{1}$$

where ideal tetrahedron is an equilateral tetrahedron with the same circumradius of the actual tetrahedron (i.e. circumradius is radius of a sphere passing through the four vertices of the tetrahedron).

The recommended interior angles range between 30° and 120° . Volumetric skew of 1 means a tetrahedral element degenerated to triangle (Fig. 6b). Volumetric skew of 0 means an ideal (equilateral) tetrahedron.

We found that, for both hexahedral and tetrahedral mesh, all poor-quality elements were located at the top or bottom (aortic bifurcation) edges of the AAA. These edges are rigidly constrained in the AAA biomechanical models (including the models created and used in this study) [13] and therefore are of limited interest for the AAA stress analysis.

2.3 Stress Computation in AAA Wall

Following our previous studies [13, 34], we used linear static finite element analysis implemented in ABAQUS/standard finite element code [35] (<https://www.3ds.com/products-services/simulia/products/abaqus/>) to calculate the AAA wall stress. This approach has been used in the freely available open-source software platform *BioPARR—Biomechanics-based Prediction of Aneurysm Rupture Risk* (<https://bioparr.mech.uwa.edu.au/>) for biomechanical analysis of AAA [13]. It relies on the observation that as patient images show the deformed (due to loading by the blood pressure) AAA geometry, the internal forces on the blood vessel wall that balance the

applied pressure can be calculated from the principles of statics [13, 34]. This implies that if the computational biomechanics simulations are set up in such a way that the deformed AAA geometry remains unchanged when loaded by blood pressure, one should obtain the stress field in the AAA wall that balances the pressure [34]. Such field is for practical purposes independent of the material properties of aorta tissue if the material is homogenous [34, 36].

For both aortic wall and ILT, we used nearly incompressible (Poisson’s ratio of 0.49) linear elastic material model. Following [15], the ILT was defined as 20 times more compliant than the AAA wall. To construct hexahedral meshes, we used hybrid 20-noded quadratic hexahedral element with reduced integration (eight integration points)—element C3D20RH in ABAQUS finite element code. For tetrahedral meshes, we used hybrid ten-noded quadratic tetrahedral element—element C3D10H in ABAQUS finite element codes. Application of hybrid formulation, that prevents volumetric locking for the nearly incompressible materials, was used.

The aneurysm was uniformly loaded at the internal surface of the ILT by the patient-specific blood pressure measured 5 minutes before acquiring the CT images [12, 37, 38]. We used mean arterial blood pressure (MAP) that is calculated from the systolic and diastolic pressures ($\text{MAP} = 1/3 \text{ systolic pressure} + 2/3 \text{ diastolic pressure}$). Top and bottom surfaces “caps” (i.e. top and bottom surfaces closing the aneurysm volume) of the aneurysm were rigidly constrained.

We analysed the maximum principal stress in the aneurysm walls as it provides indication of the internal forces within the aorta that balance the blood pressure [13]. The residual stresses in the aorta were not considered in this study as we focus on the method of generating high-quality hexahedral meshes for aneurysm wall rather than the AAA rupture assessment through stress computation.

We compared the contours of the maximum principal stress and distribution of the 99th percentile of the maximum principal stress in the aneurysm wall obtained using the hexahedral and tetrahedral finite meshes. We used 99th percentile rather the peak values to eliminate the artefacts and uncertainties due to the AAA segmentation and AAA geometry discretisation when generating the finite element meshes [39].

3 Results

3.1 Computational Grid (Finite Element Mesh) Convergence

We performed a mesh convergence study for one of the analysed AAAs (Patient 1) to ensure that computation of stress in aneurysm wall is independent of mesh size. We created three finite element models of the aneurysm of this patient using hexahedral meshes with different number of elements: Model 1 with two layers of hexahedral elements through the aneurysm wall thickness; Model 2 with three layers of hexahedral elements, and Model 3 with four layers of hexahedral. Following the approach used in BioPARR open-source software platform for biomechanical AAA

analysis, we calculated the maximum principal stress in the aneurysm wall using the linear finite element algorithm from ABAQUS/standard executed on Intel(R) Core (TM) i7-5930 K CPU @3.50 GHz with 64 GB of RAM running Windows 8 operating system. The finite element models used when analysing the mesh convergence did not include the ILT. The inner surface of the AAA wall was loaded with 12 kPa (MAP, mean arterial pressure for Patient 1).

Table 1 summarises the mesh characteristics of each studied finite element model. It also includes the peak and 99th percentile values of maximum principal stress for the three models. The peak stress values typically occur at the fixed (rigidly constrained) nodes of the top and bottom edges of the aneurysm wall, which can be regarded as a modelling artefact. Therefore, we compared 99th percentile of the maximum principal stress.

Figure 7 shows the maximum principal stress for the three studied models with respect of a percentile rank of the stress values. We refer to Fig. 7 as the maximum principal stress percentile plot. For all three models, the maximum principal stress percentile plots are very close.

Table 1 Mesh characteristics, maximum principal stress (peak value and 99th percentile), and finite element models computation time when conducting the mesh convergence analysis

	Model 1	Model 2	Model 3
No. of hexahedral elements through wall thickness	2	3	4
Element size (mm)	0.75	0.5	0.375
No. of elements	27,972	95,190	225,676
No. of nodes	154,734	477,787	1,075,083
Peak of maximum principal stress (MPa)	0.5300	0.6070	0.6831
99th percentile of maximum principal stress (MPa)	0.2700	0.2620	0.2557
Computation time (sec)	23	103	568

Fig. 7 Percentile plot of the maximum stress in the aneurysm wall of Patient 1 obtained using finite element models with different number of hexahedral elements (as indicated by the number of hexahedral elements through the aneurysm wall thickness). The results indicate that the calculated stress is mesh independent (i.e. the solution converged for two layers of hexahedral elements through the aneurysm wall thickness)

